the first specimen $\beta_0 = 198$, $\beta_1 = 434$, and for the second $\beta_0 = 348$, $\beta_1 = 764$. Thus, the assumptions adopted with respect to β_0 and β_1 are satisfied. All of the tests were carried out at pressures up to 4.0 MPa. In recording pressure value they did not differ from the limiting pressure by more than 10%. This made it possible to assume a viscosity value for methane in all tests of $\mu = 1.14 \cdot 10^{-5}$ Pa·sec (with a relative error not worse than ±0.03). Calculated permeability values for average values of the product $c^2\rho_\infty t_r$ are given in Table 1. They agree quite well with the results of steady-state measurements.

Thus, on the basis of the studies carried out it is possible to conclude that in the conditions considered the filtration process is well described by equations of an elastic regime. The method for determining filtration parameters according to typical relaxation time is new and it gives results conforming with those obtained in steady-state measurements.

LITERATURE CITED

1. S. C. Jones, "A rapid accurate unsteady-state Klinkenberg parameter," Soc. Petrol. Engrs. J., 12, No. 5 (1972).
2. D. L. Freeman and D. C. Bush, "Low permeability laboratory measurements by nonsteady-state and conventional methods," Soc. Petrol. Eng. J., 23, No. 6 (1983).
3. V. I. Goroyan, "Measurement of permeability for rock-collectors with nonsteady-state gas filtration," Tr. VNIGNI, No. 90 (1979).
4. A. G. Kovalev and V. V. Pokrovskii, "Theoretical prerequisites for determining the permeability of rocks with nonsteady-state gas filtration and possible schemes for instruments operating on this principle," Tr. VNII, NTS po Dobyche Nefti, No. 42, Nedra, Moscow (1971).
5. G. I. Barenblatt, V. M. Entov, and V. M. Ryzhik, Theory of Nonsteady-State Filtration of Liquid and Gas [in Russian], Nedra, Moscow (1972).
6. G. I. Barenblatt, V. M. Entov, and V. M. Ryzhik, Movement of Liquids and Gases in Natural Seams [in Russian], Nedra, Moscow (1984).
7. N. Dunford and J. T. Shwartz, Linear Operators. Part 2: Spectral Theory. Self-Adjoint Operators in Hilbert Space, Wiley (1958).
8. F. Riss and B. Syokefal'vi-Nad', Lectures on Functional Analysis [in Russian], Mir, Moscow (1979).

ACOUSTIC EFFECT ON THE HEAT-TRANSFER AND FLOW PARAMETERS OF A COMPOUND JET IN AN INCIDENT FLOW

A. N. Golovanov

UDC 536.24

Processes involving the interaction of small perturbations (acoustic vibrations, vibrations of a surface with gas flows), of interest in both scientific investigations and in practical applications, are encountered in problems dealing with the transition of a laminar boundary layer to a turbulent boundary layer, the sensitivity of turbulent flows to acoustic vibrations, and the control of the aerodynamic and thermal characteristics of power plants [1-3].

Here, we examine the effect of acoustic vibrations on heat transfer and the hydrodynamic parameters in a compound jet discharged from a system of circular holes counter to a free-stream flow.

Tests were conducted in jets produced by an EDP-104A-50 electric-arc plasmatron, in an ohmic gas heater, and in the working section of a T-124 low-velocity low-turbulence wind tunnel.

The models (Fig. 1), made in the form of cylinders 1, were positioned with their end counter to an incoming flow of air 2. Air 4, formed into a compound jet, was fed through the internal volume of the models and seven circular holes in the end part 3. The dynamic

Tomsk. Translated from Zhurnal Prikladnoi Mekhaniki i Tekhnicheskoi Fiziki, No. 1, pp. 153-158, January-February, 1989. Original article submitted October 6, 1987.

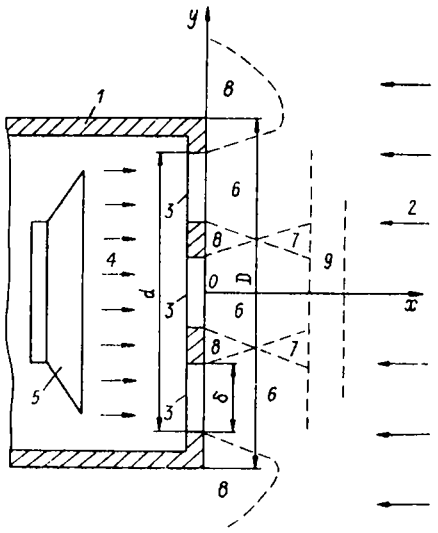

Fig. 1

loudspeaker 5 inside the model generated sinusoidal (with respect to time) longitudinal (with respect to the flow) waves which propagated along the individual jets.

Table 1 shows the geometric dimensions of the models and the test conditions. Here, T_∞ and v_∞ are the mean-mass temperature and the mean-flow-rate velocity of the incoming flow. The quantity Re_D is the Reynolds number, calculated from the diameter of the models.

The parameters of the incident flows were determined by means of thermocouples and pneumatic probes. The energy-balance conditions for the operation of the plasmatron were determined by the methods described in [4, 5]. The total rates of air flow G_w through the circular holes of the models were varied within the range $(0.1\text{-}8.5)\cdot10^{-3}$ kg/sec. The flow rates were monitored with PC and GF rotameters and were kept constant within a given test. The temperature of the air fed through the circular holes varied only slightly (300-310 K) for all tests.

During the tests, we measured the heat flow to the wall at a distance of $1\cdot10^{-3}$ m from the front critical point 0 (Fig. 1). This measurement was made by the well-known exponential method [4-6].

The parameters of the gas in the region xOy — velocity V and longitudinal u and transverse v velocity pulsations — were determined with a hot-wire anemometer (the diameter of the tungsten wire of the sensor was $20\cdot10^{-6}$ m). The values of V, u, and v were measured at 30 points with the coordinates x_i and y_j (i = 1, ...,6, j = 1, ...,5) and an interval of $5\cdot10^{-3}$ m between adjacent points (Fig. 1). The total errors of the parameter determinations were as follows: $\delta T_\infty \leqslant 10$ %, $\delta v_\infty \leqslant 6$ %, $\delta q \leqslant 9$ %, $\delta G_w \leqslant 5$ %, $\delta v \leqslant 12$ %, $\delta u \leqslant 12$ %.

The frequency and amplitude of the acoustic vibrations were established by means of a GZ acoustic vibration generator and a TA dynamic loudspeaker. The ranges of the frequency f and sound intensity I were 10-2000 Hz and 30-64 dB. The frequency parameter $F = 2\pi\nu f/v_\infty^2$ was varied within the range $33.4\cdot10^{-7}$-1.9 (ν is the kinematic viscosity of the incident flow).

Figures 2 and 3 show the dependence of the relative heat flux to the wall of the models on the frequency parameter for different rates of flow of the injected air. Here, q+ and q-

TABLE 1

Type of unit	$\delta\cdot10^{-3}$	$d\cdot10^{-3}$	$D\cdot10^{-3}$	$h\cdot10^{-3}$	T_∞, K	v_∞, m/sec	Re_D
	m						
EDP-104A-50	1	6	19	40	3600	66,1	935
Ohmic heater	1	6	19	40	460	0,51	—
T-124	12	68	120	—	300	4,34	372

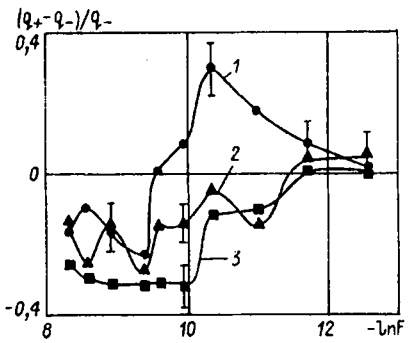

Fig. 2

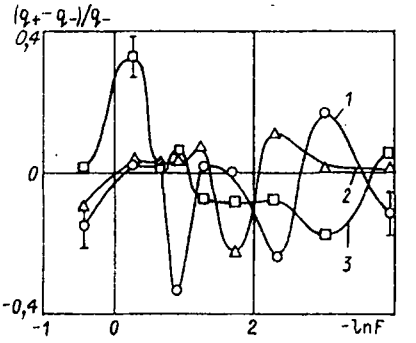

Fig. 3

are the values of heat flux in the presence and absence of the acoustic field. Curves 1-3 in Fig. 2 were obtained for the models in the plasma jet with G_w = (0.70; 1.18; 2.58)·10^{-4} kg/sec. Curves 1-3 in Fig. 3 are for the models in the jets of heated air, with G_w = (0.36; 0.62; 1.52)·10^{-4} kg/sec. The lines in Figs. 2-6 are approximations of the experimental points obtained by the least squares method.

An analysis of the results we obtained shows the dual effect of the acoustic field on heat transfer; the conditions may be such as to intensify heat transfer ($(q_+ - q_-)/q_- > 0$) or decrease the heat-transfer rate ($(q_+ - q_-)/q_- < 0$). Increases and decreases in heat-transfer rate are seen with both the plasma jet and the jet of heated air. The regions in which heat transfer is intensified are present at relatively low acoustic field frequencies and low gas injection rates (curves 1 in Figs. 1 and 2). The regions in which heat transfer is reduced are present at higher acoustic field frequencies and higher values of gas injection rate (curves 2 and 3 in Figs. 1 and 2). The sensitivity of the heat-transfer process to the frequencies associated with the acoustic field may be either stable (curves 1-3 in Fig. 2) or unstable. Here, certain groups of field frequencies stand out (curves 1-3 in Fig. 3).

To explain the increase and decrease in heat-transfer rate, we measured the profiles of velocity V and pulsations of velocity u and v in a compound jet in the working part of the wind tunnel. The rate of flow of the air injected through the circular holes was changed within the range G_2 = (4.5-8.0)·10^{-3} kg/sec. The degree of turbulence of the gas, measured on the axis of the holes at the point 0 (see Fig. 1) of the end part of the model, was 0.07-0.09.

The flow region near the wall (see Fig. 1) contains regions corresponding to the main sections of elementary jets 6, regions in which jets mix with one another 7, stagnant regions 8, and a region in which the injected gas mixes with the incident flow 9.

Curve 1 in Fig. 4 corresponds to the profile of dimensionless velocity of the gas at the distance x/δ = 1.67 from the end part of the wall of the model. The velocity of the gas at the edge of one hole here V_m = 6.78 m/sec. Curves 1 in Figs. 5 and 6 illustrate the distribution of the longitudinal u and transverse v pulsations of velocity measured at the same points as the velocity profile (curve 1 in Fig. 4): $\bar{u}^2 = \sum_{i=1}^{k} u_i^2/k$, $\bar{v}^2 = \sum_{i=1}^{k} v_i^2/k$, V_x, V_y are projections of the velocity vector. The distribution of curves 1 in Figs. 4-6 shows that high-gradient gas-velocity profiles are present on the main sections of the elementary jets. At the inflection points of the velocity profiles (y/δ = 0.42), there are large-scale low-frequency gas pulsations. The amplitude of the velocity pulsations in the stagnant zones and the zones where the elementary jets undergo mixing (y/δ = 0.83) is lower than on the main sections, while the frequency is higher.

Figure 7 shows the results of calculations of the spectral densities of the longitudinal C_{ku} and transverse C_{kv} pulsations of the gas. Curve 1 corresponds to values of C_{ku} at the point y/δ = 0.42 — the inflection point on the velocity profile — while curve 2 corresponds to the value of C_{kv} at the point y/δ = 0.83 — the point where the elementary jets merge. Such turbulent formations are termed coherent structures [2]. The results of spectral analysis shows that low-frequency large-scale turbulent pulsations of the gas develop at the inflection points, with f = 15 Hz, C_{ku} = 0.17:

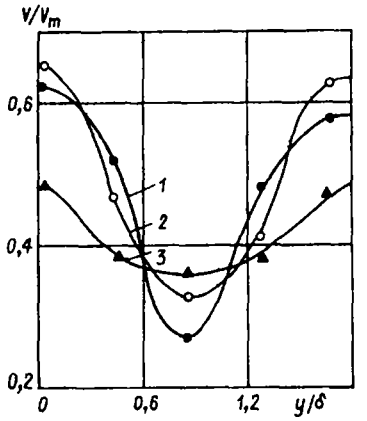

Fig. 4

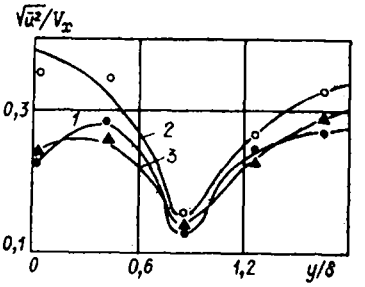

Fig. 5

$$C_{ku} = \sqrt{\left[\Delta t \sum_{i=1}^{k} \frac{u_i}{V_x} \cos(2\pi f \Delta t i)\right]^2 + \left[\Delta t \sum_{i=1}^{k} \frac{u_i}{V_x} \sin(2\pi f \Delta t i)\right]^2},$$

$$C_{kv} = \sqrt{\left[\Delta t \sum_{i=1}^{k} \frac{v_i}{V_y} \cos(2\pi f \Delta t i)\right]^2 + \left[\Delta t \sum_{i=1}^{k} \frac{v_i}{V_y} \sin(2\pi f \Delta t i)\right]^2}$$

(Δt = 0.002 sec, k = 100). In the region where the jets merge, the main contribution to the energy of the turbulent pulsations is made by transverse high-frequency pulsations $C_{\zeta v}$ = 0.14, with f = 100 Hz.

The possibility of the development of turbulent eddies in a compound jet discharged counter to a free-stream flow was indicated in [7], although here the author assumed that such eddies arise in the region where the injected gas mixes with the flow 9 (see Fig. 1), in the so-called recirculation region, or in stagnant regions 7. Our measurements show that turbulence is generated and low-frequency turbulent pulsations develop on the main sections of the elementary jets. Recirculation flows develop at a substantial distance from the wall ($x/\delta > 5$) with large rates of gas injection ($G_w > 7.3 \cdot 10^3$ kg/sec).

Curves 2 and 3 in Figs. 4–6 show the distribution of dimensionless velocity and the longitudinal and transverse pulsations of velocity measured in the section $x/\delta = 1.67$ in the presence of an acoustic field with the frequency f = 15 and 100 Hz at I = 60 dB. It is evident that the acoustic field transforms the velocity profiles in the region xOy. Low-frequency sound waves increase the amplitude of the longitudinal velocity pulsations on the main sections of the elementary jets, high-gradient regions are formed, and the velocity profiles are elongated (curves 2). High-frequency sound waves increase the amplitude of the transverse pulsations of the gas in the region where the elementary jets merge and the velocity profiles become smoother without high-gradient regions (curves 3).

The results of calculations of the cross-correlation functions [8]

$$R_{uf} = \frac{\sum_{i=1}^{k} u_i \cos 2\pi f \Delta t i}{\sqrt{\sum_{i=1}^{k} u_i^2} \sqrt{\sum_{i=1}^{k} \cos^2 2\pi f \Delta t i}}, \quad R_{vf} = \frac{\sum_{i=1}^{k} v_i \cos 2\pi f \Delta t i}{\sqrt{\sum_{i=1}^{k} v_i^2} \sqrt{\sum_{i=1}^{k} \cos^2 2\pi f \Delta t i}}$$

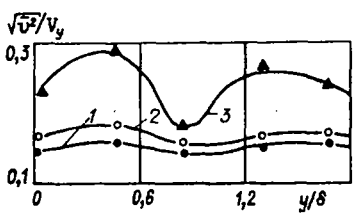

Fig. 6

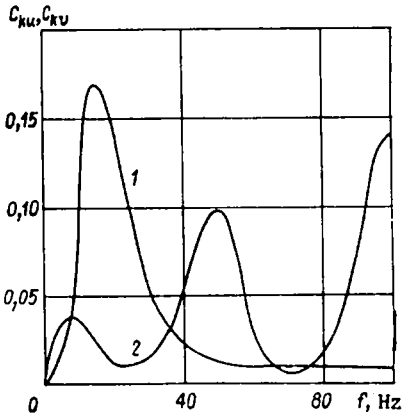

Fig. 7

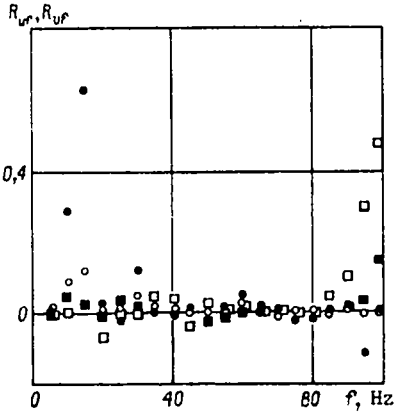

Fig. 8

are shown in Fig. 8, where the dark points correspond to the correlations of longitudinal gas pulsations in the presence of an acoustic field and sound waves. The clear points correspond to correlations of transverse pulsations of the gas in the presence of the acoustic field and sound waves. The circular points show the results of calculations at the point $y/\delta = 0.42$, while the squares show the results for the point $y/\delta = 0.83$. It is evident that low-frequency acoustic vibrations f = 15 Hz cross-correlate with the longitudinal pulsations of velocity on the main sections of the elementary jets ($y/\delta = 0.42$, $R_{uf} = 0.63$). High-frequency acoustic vibrations f = 100 Hz cross-correlate with transverse pulsations of velocity in the region where the elementary jets merge ($y/\delta = 0.83$, $R_{vf} = 0.48$).

The results of study of the parameters of the gas in a compound jet discharged counter to an incident flow showed that low-frequency acoustic vibrations promote the generation of large-scale turbulent pulsations. High-frequency acoustic vibrations suppress the formation of these pulsations and the gas flow field becomes more uniform without high velocity gradients.

The intensification of heat transfer between the models and high-temperature jets by means of low-frequency sound waves is evidently connected with the interaction of the acoustic vibrations and coherent structures on the main sections of the elementary jets. The flow is subjected to additional agitation, leading to intensification of heat transfer. High-frequency acoustic vibrations cross-correlate with transverse pulsations of velocity in the regions where the elementary jets merge. Here, large-scale pulsations of gas velocity are suppressed and heat transfer is reduced.

In conclusion, we thank S. A. Antonkin for his help in preparing and conducting the experiments and A. M. Grishin for his fruitful discussion of the results.

LITERATURE CITED

1. Yu. S. Kachanov, V. V. Kozlov, and V. Ya. Levchenko, Generation of Turbulence in a Boundary Layer [in Russian], Nauka, Novosibirsk (1981).
2. A. S. Ginevskii, E. V. Vlasov, and A. V. Kolesnikov, Aeroacoustic Interactions [in Russian], Mashinostroenie, Moscow (1978).
3. V. E. Nakoryakov, A. P. Burdukov, A. M. Boldarev, and P. P. Terleev, Heat and Mass Transfer in an Acoutic Field [in Russian], Inst. Teplofiz. Sib. Otd. Akad. Nauk SSSR, Novosibirsk (1970).
4. A. M. Grishin, V. E. Abaltusov, and A. N. Golovanov, "Experimental study of the heat and mass transfer of a plasma jet with a perforated surface in the presence of injection," Izv. Sib. Otd. Akad. Nauk SSSR Ser. Tekh. Nauk, 3, No. 15 (1980).
5. V. E. Abaltusov, A. N. Golovanov, and S. I. Al'pert, "Determination of certain parameters of a low-frequency plasma jet," in: Gasdynamics of Nonequilibrium Processes [in Russian], Inst. Teor. Prikl. Mekh. Sib. Otd. Akad. Nauk SSSR, Novosibirsk (1981).
6. Yu. V. Polezhaev and F. B. Yurevich, Thermal Protection [in Russian], Energiya, Moscow (1976).
7. J. Park, "Flow turbulence, caused by injection, in a boundary layer in the neighborhood of the critical point," Aerokosmich. Tekhnika, 2, No. 9 (1984).
8. L. E. Varankin, Theory of Compound Signals [in Russian], Sov. Radio, Moscow (1970).